

AD _____

Award Number: DAMD17-03-1-0143

TITLE: Imaging Primary Prostate Cancer and Bone Metastasis

PRINCIPAL INVESTIGATOR: Xiaoyuan Chen, Ph.D.

CONTRACTING ORGANIZATION: University of Southern California
Los Angeles, CA 90033

REPORT DATE: April 2004

TYPE OF REPORT: Annual

PREPARED FOR: U.S. Army Medical Research and Materiel Command
Fort Detrick, Maryland 21702-5012

DISTRIBUTION STATEMENT: Approved for Public Release;
Distribution Unlimited

The views, opinions and/or findings contained in this report are those of the author(s) and should not be construed as an official Department of the Army position, policy or decision unless so designated by other documentation.

REPORT DOCUMENTATION PAGE

Form Approved
OMB No. 074-0188

Public reporting burden for this collection of information is estimated to average 1 hour per response, including the time for reviewing instructions, searching existing data sources, gathering and maintaining the data needed, and completing and reviewing this collection of information. Send comments regarding this burden estimate or any other aspect of this collection of information, including suggestions for reducing this burden to Washington Headquarters Services, Directorate for Information Operations and Reports, 1215 Jefferson Davis Highway, Suite 1204, Arlington, VA 22202-4302, and to the Office of Management and Budget, Paperwork Reduction Project (0704-0188), Washington, DC 20503

1. AGENCY USE ONLY
(Leave blank)

2. REPORT DATE
April 2004

3. REPORT TYPE AND DATES COVERED
Annual (1 Apr 2003 - 31 Mar 2004)

4. TITLE AND SUBTITLE

Imaging Primary Prostate Cancer and Bone Metastasis

5. FUNDING NUMBERS

DAMD17-03-1-0143

6. AUTHOR(S)

Xiaoyuan Chen, Ph.D.

7. PERFORMING ORGANIZATION NAME(S) AND ADDRESS(ES)

University of Southern California
Los Angeles, CA 90033

E-Mail: xchen@usc.edu

8. PERFORMING ORGANIZATION
REPORT NUMBER

9. SPONSORING / MONITORING
AGENCY NAME(S) AND ADDRESS(ES)

U.S. Army Medical Research and Materiel Command
Fort Detrick, Maryland 21702-5012

10. SPONSORING / MONITORING
AGENCY REPORT NUMBER

11. SUPPLEMENTARY NOTES

20041028 094

12a. DISTRIBUTION / AVAILABILITY STATEMENT

Approved for Public Release; Distribution Unlimited

12b. DISTRIBUTION CODE

13. ABSTRACT (Maximum 200 Words)

The **overall objective** of the proposed research is to develop positron emitter labeled bombesin analogs with high affinity for the GRP receptor BB2 for microPET imaging of both androgen dependent and androgen independent prostate cancer xenografted mice. **Specific Aims:** (1) Design, synthesize, and characterize positron emitting bombesin analogs, labeled with copper-64 or fluorine-18; (2) Conduct *in vitro* studies of copper-64 and fluorine-18 labeled bombesin analogs to evaluate the effect of modification and radiolabeling on the receptor binding affinity and specificity; (3) Evaluate *in vivo* efficacy of these novel radiopharmaceuticals in the murine PC-3 and CWR22 human prostate cancer xenograft models. **Major Findings:** We conjugated DOTA with Lys³-bombesin and labeled this compound with ⁶⁴Cu. The radiotracer ⁶⁴Cu-DOTA-[Lys³]BBN revealed high affinity and specificity for androgen independent PC-3 prostate cancer cells. Significant activity accumulation in GRPR positive PC-3 tumor and pancreas were observed. MicroPET and autoradiographic imaging of the radiotracer in athymic nude mice bearing subcutaneous PC-3 and CWR22 tumors showed strong tumor-to-background contrast. This study demonstrates that ⁶⁴Cu-DOTA-[Lys³]BBN is able to detect GRPR-positive prostate cancer by PET imaging. Further studies to evaluate the metabolic stability and optimization of the radiotracers for prolonged tumor retention and improved *in vivo* kinetics is in progress.

14. SUBJECT TERMS

Prostate Cancer; Radionuclide imaging; Positron Emission Tomography, Bombesin, Cu-64

15. NUMBER OF PAGES
53

16. PRICE CODE

17. SECURITY CLASSIFICATION
OF REPORT
Unclassified

18. SECURITY CLASSIFICATION
OF THIS PAGE
Unclassified

19. SECURITY CLASSIFICATION
OF ABSTRACT
Unclassified

20. LIMITATION OF ABSTRACT
Unlimited

Table of Contents

Cover.....	1
SF 298.....	2
Introduction.....	3
Body.....	4
Key Research Accomplishments.....	7
Reportable Outcomes.....	8
Conclusions.....	9
References.....	10
Appendices.....	11

INTRODUCTION

Although GRP receptors are known to be overexpressed in human neoplastic prostate tissues, little has been published on the development of radiopharmaceuticals for systemic evaluation of GRP receptor agonists and antagonists. The overall objective of the proposed research is to develop positron emitter labeled bombesin analogs with high affinity for the GRP receptor BB2 for microPET imaging of both androgen dependent and androgen independent prostate cancer xenografted mice. **Specific Aims:** (1) Design, synthesize, and characterize positron emitting bombesin analogs, labeled with copper-64 or fluorine-18; (2) Conduct *in vitro* studies of copper-64 and fluorine-18 labeled bombesin analogs to evaluate the effect of modification and radiolabeling on the receptor binding affinity and specificity; (3) Evaluate *in vivo* efficacy of these novel radiopharmaceuticals in the murine PC-3 and 22Rv1 human prostate cancer xenograft models.

BODY

Lys³-bombesin ([Lys³]BBN) was conjugated with 1,4,7,10-tetraazadodecane-*N,N',N'',N'''*-tetraacetic acid (DOTA) and labeled with positron emitter ⁶⁴Cu (**Fig. 1**). Specific activity of ⁶⁴Cu-DOTA-[Lys³]BBN ranged from 400 to 1,000 Ci/mmol (15-38 GBq/μmol). Competitive receptor binding assay using PC-3 cells against ¹²⁵I-[Tyr⁴]BBN revealed an IC₅₀ value of 2.2±0.5 nM for DOTA-[Lys³]BBN. Incubation of the ⁶⁴Cu-labeled radiotracer showed temperature- and time-dependent internalization.

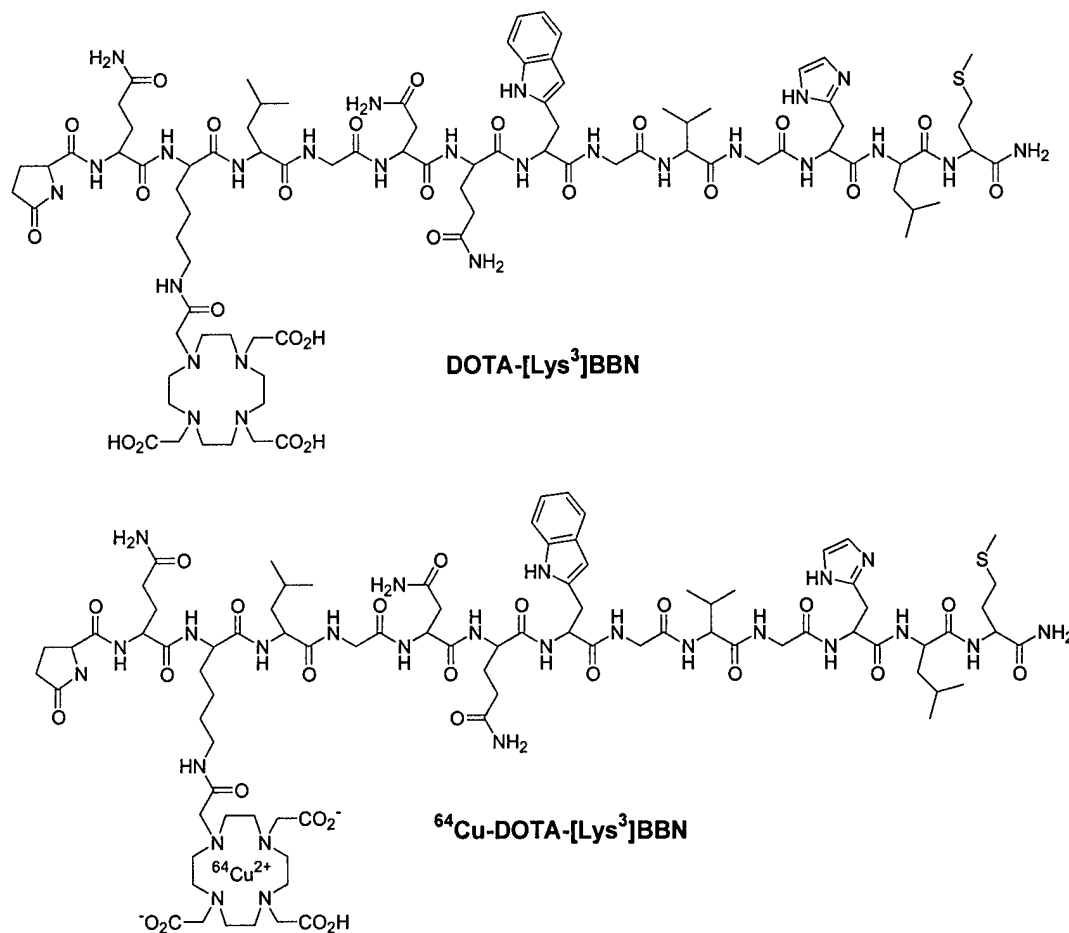


Figure 1. Schematic structures of DOTA-[Lys³]BBN conjugate and ⁶⁴Cu-DOTA-[Lys³]BBN.

The radiotracer revealed higher uptake in AI PC-3 tumor (5.62±0.08 %ID/g at 30 min p.i.) than in AD CWR22 tumor (1.75±0.05 %ID/g at 30 min p.i.). Significant accumulation of the activity in GRPR positive pancreas was also observed (10.4±0.15 %ID/g at 30 min p.i.) (**Fig. 2**). Co-injection of blocking dose of [Lys³]BBN inhibited the activity accumulation in PC-3 tumor and pancreas but not in CWR22 tumor (**Fig. 3**). MicroPET and autoradiographic imaging of ⁶⁴Cu-DOTA-[Lys³]BBN in athymic nude mice bearing subcutaneous PC-3 and 22Rv1 tumors showed strong tumor-to-background contrast (**Fig. 4**). The uptake indices found with microPET and QAR for PC-3 tumor and pancreas were significantly lower than those obtained from direct tissue sampling (**Fig.**

5). It is possible that partial self-inhibition of receptor specific uptake in PC-3 tumor, pancreas and other tissues that express the GRP receptor occurred during the imaging studies. Conversely, the inability to inhibit CWR22 tumor activity accumulation in the imaging study is consistent with the known low GRP receptor expression in androgen-dependent tumors such as CWR22.

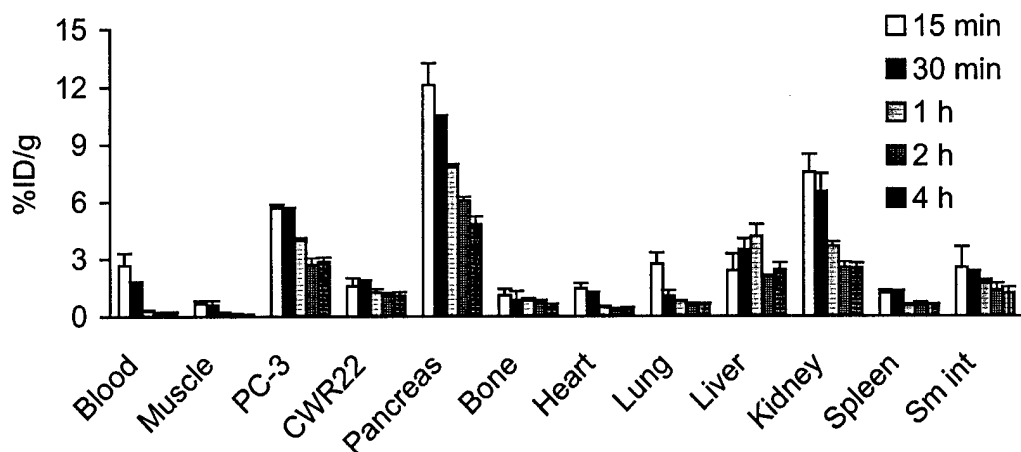


Figure 2. Biodistribution of ^{64}Cu -DOTA-[Lys³]BBN in male athymic nude mice bearing s.c. PC-3 (AI) and CWR22 (AD) tumors. Mice were intravenously injected with 10 μCi of radioligand and sacrificed at 15 min, 30 min, 1 h, 2 h and 4 h. The data are presented as mean % ID/g \pm SD (n = 4). Sm int = small intestine.

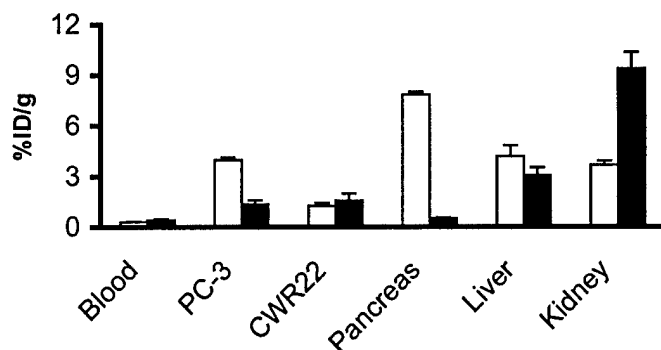


Figure 3. Receptor blocking study: biodistribution of ^{64}Cu -DOTA-[Lys³]BBN at 1 h time point without (white bars) and with (black bars) co-injection of 200 μg of BBN to determine GRP receptor specific binding. Significant inhibition of activity accumulation in PC-3 tumor ($p < 0.001$) and pancreas ($p < 0.001$) were observed. Data are presented as mean % ID/g \pm SD in reference to total injected dose of the radiotracer (n = 4 for each group).

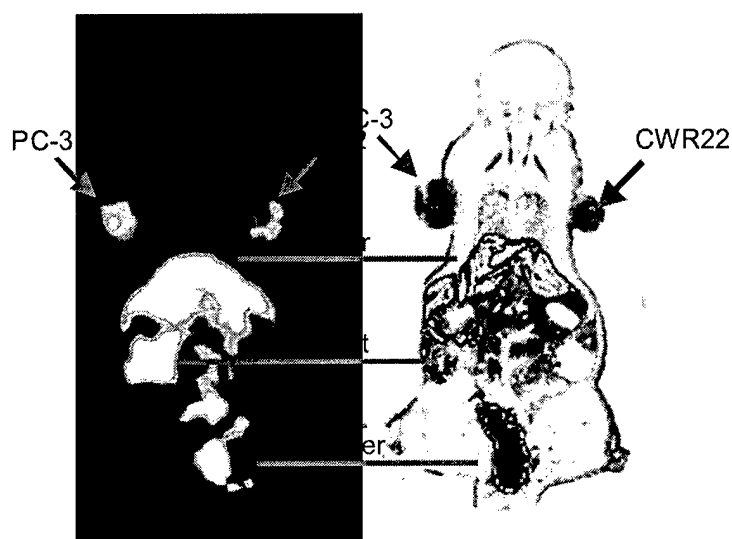


Figure 4. Left: Coronal microPET image of tumor bearing mouse (PC-3 on the right shoulder and CWR22 on the right shoulder) 1 h after administration of ^{64}Cu -DOTA-[Lys³]BBN. Right: Digital autoradiograph of the section containing tumors.

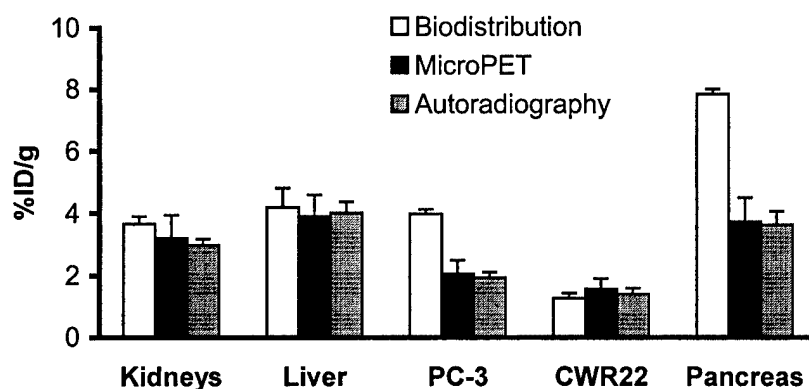


Figure 5. Kidney, liver, PC-3 tumor and CWR22 tumor uptake comparison as obtained from traditional biodistribution ($n = 4$), microPET ($n = 3$), and autoradiographic quantification ($n = 3$). Quantification of microPET and autoradiography revealed similar activity accumulation in both PC-3 tumor and pancreas, which were both lower than those obtained from biodistribution study.

KEY RESEARCH ACCOMPLISHMENTS

- [Lys³]bombesin was labeled with positron emitter copper-64 ($t_{1/2} = 12.8$ h) with high specific activity;
- Subcutaneous PC-3 (AR-) and CWR22 (AR-) tumor models developed in female athymic nude mice;
- The radiotracer ⁶⁴Cu-DOTA-[Lys³]BBN indicated GRP receptor specific uptake in PC-3 tumor and pancreas;
- MicroPET and autoradiographic imaging of ⁶⁴Cu-DOTA-[Lys³]BBN in athymic nude mice bearing subcutaneous PC-3 and CWR22 tumors showed strong tumor-to-background contrast.

REPORTABLE OUTCOMES

Based upon the results obtained from this funding, a manuscript was accepted by J. Nucl. Med., and one abstract submitted to the Academy of Molecular Imaging was accepted for oral presentation.

Chen X, Park R, Hou Y, Tohme M, Shahinian AH, Bading JR, Conti PS
MicroPET and Autoradiographic Imaging of GRP Receptor Expression with ^{64}Cu -DOTA-[Lys³]bombesin in Human Prostate Adenocarcinoma Xenografts
J. Nucl. Med. 2004; 45: 000-000

Chen X, Hou Y, Park R, Tohme M, Shahinian AH, Bading JR, Conti PS
Evaluation of ^{64}Cu -Labeled [Lys³]Bombesin as PET Tracer for Prostate Cancer GRP Receptor Imaging.
AMI International Conference 2004, Orlando, FL, March, 2004.

CONCLUSIONS

Overall, we have successfully labeled [Lys³]BBN with positron emitter Cu-64 for microPET imaging of subcutaneous PC-3 prostate cancer tumor bearing athymic nude mice with good tumor to contralateral background ratio. However, prominent liver and kidney activity accumulation of this radiotracer is problematic. Further studies are needed to optimize the radiotracer for prolonged tumor retention and improved in vivo kinetics. For the remaining two years of the funding period, a series of bombesin analogs will be labeled with F-18 and Cu-64 and evaluated for their receptor targeting abilities both in vitro and in vivo.

REFERENCES

N/A

APPENDICES

1. J. Nucl. Med. Manuscript.
2. 2004 AMI conference abstract

**MicroPET and Autoradiographic Imaging of GRP Receptor Expression
with ^{64}Cu -DOTA-[Lys³]bombesin in Human Prostate Adenocarcinoma
Xenografts**

Xiaoyuan Chen, Ryan Park, Yingping Hou, Michel Tohme, Antranik H. Shahinian,
James R. Bading, Peter S. Conti

*PET Imaging Science Center, University of Southern California Keck School of
Medicine, Los Angeles, CA 90033*

*** Correspondence Should be Sent to:**

Peter S. Conti, M.D., Ph.D.
Department of Radiology
University of Southern California
1510 San Pablo St., Suite 350
Los Angeles, CA 90033
Tel: (323)442-5940
Fax: (323)442-3253
Email: pconti@usc.edu

Running Title: PET Imaging of Prostate Cancer GRP Receptor

Keywords: prostate cancer, microPET, GRP receptor, bombesin, copper-64.

Word count: 6280

ABSTRACT

Overexpression of gastrin-releasing peptide (GRP) receptor in both androgen-dependent (AD) and androgen-independent (AI) human neoplastic prostate tissues provides an attractive target for prostate cancer imaging and therapy. The goal of this study is to develop ^{64}Cu -radiolabeled GRP analogs for positron emission tomography (PET) imaging of GRPR expression in prostate cancer xenografted mice.

Methods: Lys³-bombesin ([Lys³]BBN) was conjugated with 1,4,7,10-tetraazadodecane-*N,N',N'',N'''*-tetraacetic acid (DOTA) and labeled with the positron emitting isotope ^{64}Cu ($t_{1/2} = 12.8$ h, 19% β^+). Receptor binding of DOTA-[Lys³]BBN and internalization of ^{64}Cu -DOTA-[Lys³]BBN by PC-3 prostate cancer cells were measured. Tissue biodistribution, microPET and whole-body autoradiographic imaging of the radiotracer were also investigated in PC-3 (androgen-independent)/CRW22 (androgen-dependent) prostate cancer tumor models.

Results: A competitive receptor binding assay using ^{125}I -[Tyr⁴]BBN against PC-3 cells yielded an IC_{50} value of 2.2 ± 0.5 nM for DOTA-[Lys³]BBN. Incubation of cells with the ^{64}Cu -labeled radiotracer showed temperature- and time-dependent internalization. At 37°C more than 60% of the tracer was internalized within the first 15 min and uptake remained constant for 2 h. Radiotracer uptake was higher in AI PC-3 tumor (5.62 ± 0.08 %ID/g at 30 min p.i.) than in AD CWR22 tumor (1.75 ± 0.05 %ID/g at 30 min p.i.). Significant accumulation of the activity in GRPR positive pancreas was also observed (10.4 ± 0.15 %ID/g at 30 min p.i.). Co-injection of a blocking dose of [Lys³]BBN inhibited the activity accumulation in PC-3 tumor and pancreas, but not in CWR22 tumor. MicroPET and autoradiographic imaging of ^{64}Cu -DOTA-[Lys³]BBN in athymic

nude mice bearing subcutaneous PC-3 and CWR22 tumors showed strong tumor-to-background contrast.

Conclusion: This study demonstrates that PET imaging of ^{64}Cu -DOTA-[Lys³]BBN is able to detect GRPR-positive prostate cancer.

Keywords: prostate cancer, microPET, GRP receptor, bombesin, copper-64.

INTRODUCTION

Positron emission tomography (PET) is a high-resolution and high-sensitivity nuclear medicine technique utilizing radiopharmaceuticals that depict physiological, metabolic, and molecular processes in vivo. The most widely used agent is ^{18}F -fluoro-deoxyglucose (FDG), which accumulates in cells that have an increased metabolism either due to increased need for and/or an inefficient glucose metabolism, such as cancer. Although FDG-PET has been shown to effectively detect many types of primary tumors and metastases, it is not able to reliably differentiate benign hyperplasia (BHP) and prostate cancer (1) or even to detect organ-confined carcinoma (2). Uptake of FDG in prostate carcinoma is generally low, apparently because the glucose utilization of prostate carcinoma cells is not enhanced significantly enough (compared to normal cells) to allow delineation of the tumor on the PET scan. Recent investigations of ^{11}C (3,4) and ^{18}F (5-8) labeled choline, and ^{11}C -acetate (9-12) indicate that these agents hold promise in this disease. High expression of receptors on prostate cancer cells, as compared with normal prostate tissue and peripheral blood cells, provides the molecular basis for using radiolabeled receptor agonists or antagonists to visualize prostate tumors in nuclear medicine. Fluorine-18 labeled androgens have been used to identify androgen-positive tissue in primates (13). While this method is useful in determining if prostate cancer is hormone dependent, it does not provide a means for detecting tumors that are hormone independent. Thus, new markers able to identify the molecular determinants of prostate cancer development and progression regardless of androgen dependence need to be investigated.

The G protein-coupled gastrin-releasing peptide (GRP) receptor, mediates the diverse actions of mammalian bombesin (BBN) related peptide, GRP. In addition to its natural presence in the central nervous system and peripheral tissues, GRP receptor is overexpressed in a number of neuroendocrine tumors including prostate cancer (14,15). In vitro receptor autoradiography of human non-neoplastic and neoplastic prostate tissue sections with ^{125}I -[Tyr⁴]bombesin as radioligand indicated high density of GRPR in well differentiated carcinomas as well as bone metastases, but little or no GRP receptor was found in hyperplastic prostate and glandular tissue. This suggests that GRP receptor may be an indicator of early molecular events in prostate carcinogenesis and may be useful in differentiating prostate hyperplasia from neoplasia (14,15). GRP receptor specific binding of ^{125}I -[Tyr⁴]bombesin was observed in human prostate cancer cell lines that are androgen-independent (AI) but not in those that are androgen-dependent (AD) (16). GRP promotes the growth and invasiveness of prostate cancer in vitro, and its secretion in vivo by endocrine cells is thought to be partially responsible for AI progression of the disease (17) by transactivation and up-regulation of epidermal growth factor (EGF) receptors (18). Therefore, the use of GRPR antagonists and/or GRPR-targeting cytotoxic peptide conjugates could be an effective chemotherapeutic approach (19). In nuclear medicine, suitably radiolabeled bombesin analogs have great potential for early noninvasive diagnosis as well as radiotherapy of prostate cancer (20,21).

Gamma-emitting (γ) $^{99\text{m}}\text{Tc}$ labeled bombesin analogs have been synthesized and evaluated in vivo in normal mice (22,23) and PC-3 tumor-bearing mice (24,25), and have undergone feasibility testing in human patients (21). Although γ emitters currently are

more readily available relative to positron (β^+) emitting radionuclides, the sensitivity of PET is at least 1-2 orders of magnitude better than that of single photon imaging systems (26). The acquisition of higher count statistics permits detection of smaller tumors for a given amount of radioactivity.

Recently Rogers et al (27) labeled DOTA-Aoc-BBN(7-14) with ^{64}Cu and applied this radiotracer to subcutaneous PC-3 xenografts. Although the tumor was well visualized, however, the sustained blood concentration and persistent liver and kidney retention limited potential clinical application of this tracer. In the present work, we evaluated the DOTA-[Lys³]BBN conjugate complexed with ^{64}Cu for in vitro receptor binding assay in PC-3 cells, for tumor targeting and in vivo kinetics by direct tissue sampling, and for visualization of prostate cancer tumors by microPET and whole-body autoradiography.

Materials and Methods

Chemistry and Radiochemistry

[Lys³]bombesin ([Lys³]BBN, American Peptide, Inc., San Jose, CA) was conjugated with 1,4,7,10-tetraazadodecane-*N,N',N'',N'''*-tetraacetic acid (DOTA) via *in situ* activation and coupling. Typically, DOTA, 1-ethyl-3-[3-(dimethylamino)propyl]carbodiimide (EDC), and *N*-hydroxysulfonosuccinimide (SNHS) at a molar ratio of DOTA : EDC : SNHS = 10 : 5 : 4 were mixed and reacted at 4°C for 30 min (pH = 5.5). The sulfosuccinimidyl ester of DOTA (DOTA-OSSu) prepared above without purification was then reacted with [Lys³]BBN in a theoretical stoichiometry of 5:1 and allowed to stand at 4°C overnight (pH 8.5-9.0). The DOTA-[Lys³]BBN conjugate was then purified by semi-preparative HPLC using a Waters 515 chromatography system with a Vydac protein and peptide column (218TP510, 5 µm, 250 × 10 mm). The flow was 3 mL/min, with the mobile phase starting from 95% solvent A (0.1% TFA in water) and 5% solvent B (0.1% TFA in acetonitrile) (0-2 min) to 35% solvent A and 65% solvent B at 32 min. The peak containing the DOTA conjugate was collected, lyophilized, and dissolved in H₂O at a concentration of 1 mg/mL for use in radiolabeling reactions. Analytical HPLC was performed on the same pump system using a Vydac 218TP54 column (5 µm, 250 × 4.6 mm) and flow rate of 1 mL/min.

Copper-64 was produced on a CS-15 biomedical cyclotron at Washington University School of Medicine. The DOTA-[Lys³]BBN conjugate was labeled with ⁶⁴Cu by addition of 1-5 mCi of ⁶⁴Cu (2-5 µg DOTA-[Lys³]BBN conjugate per mCi ⁶⁴Cu) in 0.1 N NaOAc (pH 5.5) buffer followed by 45 min incubation at 50°C. The reaction was

terminated by adding 5 μ L of 10 mM EDTA solution and radiochemical yield was determined by Radio-TLC using Whatman MKC18F TLC plates as the stationary phase and 70:30 MeOH:10% NaOAc as the eluent. ^{64}Cu -DOTA-RGD was purified on a C-18 SepPak cartridge, using 85% ethanol as the elution solvent. Radiochemical purity was determined by radio-TLC or radio-HPLC. The ethanol was evaporated and the activity was reconstituted in phosphate-buffered saline and passed through a 0.22 μ m Millipore filter into a sterile multidose vial for *in vitro* and animal experiments.

In Vitro Receptor Binding Studies.

In vitro GRP receptor binding affinities and specificities of the DOTA-[Lys³]BBN conjugate were assessed via displacement cell-binding assays using ^{125}I -[Tyr⁴]BBN (Perkin-Elmer Life Sciences Products, Inc., Boston, MA) as the GRP receptor specific radioligand. Experiments were performed on PC-3 (androgen-independent) human prostate cancer cells (ATCC, Manassas, VA) by modification of a method previously described (25). Briefly, cells were grown in Ham's F-12K medium supplemented with 10% fetal bovine serum (FBS). PC-3 cells were harvested and seeded in 24-well plates at 10^5 cells per well. Twenty-four hours later, the cells were washed twice with binding buffer containing 50 mM HEPES, 125 mM NaCl, 7.5 mM KCl, 5.5 mM MgCl_2 , 1 mM EGTA, 2 mg/mL BSA, 2 mg/L chymostatin, 100 mg/L soybean trypsin inhibitor, and 50 mg/L bacitracin at pH 7.4 and then incubated for 1 h at 37°C with 20,000 cpm of ^{125}I -[Tyr⁴]BBN (specific activity: 2,000 Ci/mmol) in the presence of increasing concentrations of DOTA-[Lys³]BBN conjugate ranging from 0 to 2,000 nM. After incubation, the cells were washed twice with binding buffer and solubilized with 1 N

NaOH and activity was measured in a γ -counter (Packard). The IC_{50} value for the displacement binding of ^{125}I -[Tyr⁴]BBN by DOTA-[Lys³]BBN conjugate was calculated by non-linear regression analysis using the GraphPad PrismTM computer fitting program (GraphPad Software, Inc., San Diego, CA). Experiments were done twice with triplicate samples.

Internalization Studies

Internalization of ^{64}Cu -DOTA-[Lys³]BBN was measured by modifying a previously described technique (25). Briefly, PC-3 (androgen independent) cells were incubated in triplicate in 6-well plates with about 200,000 cpm of ^{64}Cu -labeled tracer with or without an excess of 1 μM bombesin for 2 h at 4 °C. After the preincubation, cells were washed with ice-cold binding buffer to remove free radioligand and then incubated with previously warmed binding buffer at 37 °C for 0, 15, 30 and 120 min for internalization. The percentage of ^{64}Cu activity trapped in the cells was determined after removing ^{64}Cu activity bound to the cell surface by washing twice with acid (50 mM glycine and 0.1 M NaCl, pH 2.8). Cells were then solubilized by incubating with 1 N NaOH and counted to determine internalized radioligand.

Biodistribution

Human prostate cancer carcinoma xenografts were induced by subcutaneous injection of 10^7 PC-3 (androgen-independent) cells to the left front leg and 10^7 CWR22 (androgen-dependent) cells to the right front leg of 4-6 week old male athymic nude mice (Harlan, Indianapolis, IN). Three to 4 weeks later, when the tumors reached 0.4-0.6 cm

diameter, the mice were injected with 10 μCi of DOTA-[Lys³]BBN intravenously into the tail vein. Mice ($n = 4$ per time point) were sacrificed by cervical dislocation at different time points post-injection (p.i.). Blood, tumor and the major organs and tissues were collected, wet-weighed, and counted in a γ -counter (Packard). The percent injected dose per gram (%ID/g) was determined for each sample. For each mouse, radioactivity of the tissue samples was calibrated against a known aliquot of the injectate. Values are quoted as mean \pm standard deviation (SD). The receptor-mediated localization of the radiotracers was investigated by determining the biodistribution of radiolabeled peptide in the presence of 1 mg/kg and 10 mg/kg of BBN at 1 h p.i. ($n = 4$).

MicroPET Imaging

Positron emission tomography (PET) imaging was performed on a microPET R4 rodent model scanner (Concorde Microsystems Inc, Knoxville, TN). The scanner has a computer-controlled bed, 10.8 cm transaxial and 8 cm axial field of view (FOV). It has no septa and operates exclusively in 3 D list mode. All raw data were first sorted into 3D sinograms, followed by Fourier rebinning and 2D filtered back projection image reconstruction using a ramp filter with the Nyquist limit (0.5 cycles/voxel) as the cut-off frequency. For PET imaging of prostate cancer-bearing mice, the animals were injected with 400 μCi ⁶⁴Cu-DOTA-[Lys³]BBN via the tail vein. The mouse was then euthanized at 1 h p.i. and placed near the center of the FOV of the microPET, where the highest image resolution and sensitivity are available. Static imaging was performed for 20 min ($n = 3$). For receptor blocking experiment, one mouse bearing PC-3 tumor on the right front leg was imaged (20 min static scan at 1 h postadministration of 400 μCi ⁶⁴Cu-

DOTA-[Lys³]BBN) twice two days apart: (a) without co-injection with BBN; (b) with 10 mg/kg BBN. No attenuation correction was applied to the microPET scans. Instead, the attenuation correction factors were incorporated into the system calibration. In brief, a vial with similar volume (30 mL, 5 cm in diameter) to a nude mouse body was filled with a known amount of ⁶⁴CuCl₂ and scanned for 1 h. The static scan was reconstructed with the FBP protocol and the count rate from the images of the phantom was compared with the known activity concentration to obtain a system calibration factor. With this approach, uptake index (= ROI (μCi/mL)/injected dose (μCi) × 100%) of tissues and organs of interest were consistent with the % ID/g value obtained from direct tissue sampling after the microPET imaging. The error was within 5-10%.

Whole-Body Autoradiography

Autoradiography was performed using a Packard Cyclone Storage Phosphor Screen system (Downers Grove, IL) and a Bright 5030/WD/MR cryomicrotome (Hacker Instruments, Fairfield, NJ). Immediately after microPET scanning, the mice were frozen in a dry ice and isopropyl alcohol bath for two minutes. The bodies were then embedded in a 4% carboxymethyl cellulose (CMC) (Aldrich, Milwaukee, WI) in water mixture using a stainless steel and aluminum mold. The mold was placed in the dry ice and isopropyl alcohol bath for five minutes and then into a -20°C freezer for one hour. The walls of the mold were removed, and the frozen block was mounted in the cryomicrotome. The block was cut into 50 μM sections, and desired sections were digitally photographed and captured for autoradiography. The sections were transferred into a chilled autoradiography cassette containing a Super Resolution screen (Packard,

Meriden, CT) and kept there overnight at -20°C. Screens were read with the Packard Cyclone laser scanner. Quantification of autoradiographic images was validated by a direct tissue sampling technique. In brief, 50 micron slices of tumor tissue were cut and exposed to Super Resolution Screen for 24 h, the ROIs drawn from the autoradiographs were described as detector light units (DUL) per mm² and correlated with direct gamma counter assays of the tissue samples scooped out of the frozen block (n = 3). A linear relationship between tissue %ID/g and autoradiography image intensity was obtained, and the conversion factor thus obtained was thus used for autoradiography quantification.

Statistic Analysis.

The data were expressed as means \pm SD. One-way analysis of variance (ANOVA) was used for statistical evaluation. Means were compared using Student's *t*-test. *P* values < 0.05 were considered significant.

RESULTS

Synthesis and Radiolabeling

The DOTA-[Lys³]BBN conjugate (**Figure 1**) was produced in 75% yield after HPLC purification. The retention time of this compound on HPLC was 18.5 min, whereas [Lys³]BBN eluted at 19.2 min under the same conditions. MALDI-TOF-MS: m/z = 1976 for $[M+H]^+$ ($C_{87}H_{137}N_{26}O_{26}S$), 1998 for $[M + Na]^+$, and 2014 for $[M + K]^+$. ⁶⁴Cu-DOTA-[Lys³]BBN was labeled in $\geq 90\%$ radiochemical yield and $\geq 98\%$ radiochemical purity, and was used immediately for *in vitro* and *in vivo* assays. Free ⁶⁴Cu-acetate remained at the origin of the radio-TLC plate and R_f value of ⁶⁴Cu-DOTA-[Lys³]BBN was about 0.5. Specific activity of ⁶⁴Cu-DOTA-RGD ranged from 400 to 1,000 Ci/mmol (15-38 GBq/ μ mol).

In Vitro Receptor Binding Assay

The binding affinity of DOTA-[Lys³]BBN conjugate for GRP receptor was tested for androgen-independent human prostate cancer PC-3 cells. As seen in **Figure 2**, the data show a typical sigmoid curve for the displacement of ¹²⁵I-[Tyr⁴]BBN from PC-3 cells as a function of increasing concentrations of the DOTA-[Lys³]BBN conjugate. The IC₅₀ value was determined to be 2.2 ± 0.5 nM. In the absence of DOTA-[Lys³]BBN competitor, approximately 10% of added ¹²⁵I-[Tyr⁴]BBN was bound. Only about 1% of added radioligand was bound to the cells in the presence of 1 μ M of DOTA-[Lys³]BBN, suggesting that 90% of bound ¹²⁵I-[Tyr⁴]BBN was GRP receptor specific.

The internalization of ^{64}Cu -DOTA-[Lys³]BBN into PC-3 cells is described in **Figure 3**.

The rate of internalization was time and temperature dependent. At 4°C, cell surface binding occurred but internalization was minimal (< 10%). Incubation at 37°C showed rapid internalization rate with 65 ± 10 % of radioactivity internalized by 30 min.

Biodistribution Studies

Summary of the biodistribution data for ^{64}Cu -DOTA-[Lys³]BBN in PC-3/CWR22 tumor-bearing mice is shown in **Figure 4**. This radiotracer had rapid blood clearance with only 0.30 ± 0.04 %ID/g remaining in the circulation at 1 h with further decrease at 2 h and 4 h time points. Tumor-to-blood ratios at 1 h were 13.1 ± 2.3 and 4.1 ± 1.3 for PC-3 and CWR22 tumors, respectively. Liver uptake reached maximum at 1 h (4.18 ± 0.63 %ID/g) and declined to 2.09 ± 0.5 %ID/g at 2 h p.i. The rapid decrease of activity accumulation in the kidneys suggests a predominant renal clearance pathway of this radiotracer. A significant uptake of ^{64}Cu -DOTA-[Lys³]BBN in the GRP receptor-bearing pancreas was observed (10.4 ± 0.14 %ID/g at 30 min after injection and 6.08 ± 0.18 %ID/g after 2 h). Results indicated GRP receptor specific uptake in PC-3 tumor and pancreas (**Figure 5**), which was confirmed by the receptor blocking study at 1 h time point as the uptake in these tissues were effectively inhibited upon co-injection of 10 mg/kg BBN (7.83 ± 0.52 %ID/g vs. 0.52 ± 0.05 %ID/g for pancreas, $p < 0.001$; 3.97 ± 0.15 %ID/g vs. 1.35 ± 0.24 %ID/g for PC-3 tumor, $p < 0.001$). Co-injection of 1 mg/kg BBN resulted in partial inhibition of activity accumulation in PC-3 tumor (2.08 ± 0.35 %ID/g) and pancreas (2.75 ± 0.43 %ID/g). Activity accumulation in the androgen-dependent CWR22 tumor was not affected by the administration of BBN. No significant

changes of uptake in other normal organs were seen except for the kidneys, which had increased uptake in the blocked vs. the control mice ($p < 0.01$), presumably due to decreased specific binding in tissues.

MicroPET and Autoradiographic Imaging

The localization of ^{64}Cu -DOTA-[Lys³]BBN in PC-3/CWR22 tumor-bearing mice as determined by microPET imaging followed by whole-body autoradiography is depicted in **Figure 6**. On the left is a coronal image of a tumor-bearing mouse 1 h after administration of 400 μCi of ^{64}Cu -DOTA-[Lys³]BBN. The microPET image is concordant with a whole-body autoradiographic section seen on the right. Both PC-3 (left) and CWR22 (right) tumors were visible with clear contrast from the adjacent background. Prominent uptake was also observed in the liver and kidneys, and clearance of the activity through the urinary bladder is evident. Uptake indices at 1 h derived from microPET (tail vein injection of 400 μCi activity) and quantitative autoradiography (QAR) are compared with data obtained from direct tissue sampling (tail vein injection of 10 μCi activity) in **Figure 7**. The results from microPET ROI analysis agreed with the results obtained from autoradiographic quantification for the organs and tissues examined. It is noticeable that PC-3 tumor and pancreas uptake obtained from microPET and QAR were significantly lower than those obtained from the direct biodistribution measurement. **Figure 8** shows transaxial microPET images of PC-3 tumor-bearing nude mouse, 1 h after administration of ^{64}Cu -DOTA-[Lys³]BBN, with and without a co-injection of 10 mg/kg BBN. There is a clear visualization of the PC-3 tumor in the animal

on the left without the presence of competitor. Conversely, the same mouse that received a blocking dose of BBN showed reduced tracer localization in the tumor.

DISCUSSION

This study showed that suitably labeled bombesin analogs can be used to image both androgen-independent (AI) and androgen-dependent (AD) prostate cancer in preclinical animal models. In particular, this study demonstrated that AI PC-3 but not AD CWR22 prostate cancer tumor has GRP receptor specific activity accumulation.

The overexpression of peptide receptors in human tumors is of considerable interest for tumor imaging and therapy. Because of their small size, peptides have faster blood clearance and higher target-to-background ratios compared to macromolecular compounds. Radiolabeled receptor-binding peptides have recently emerged as a new class of radiopharmaceuticals. Various peptides have been used for tumor scintigraphy. For example, somatostatin receptors, which are highly expressed in most neuroendocrine tumors, have been targeted successfully for both imaging and therapy with octreotide. The long-term treatment of patients with octreotide has been successful in relieving the symptoms resulting from excessive hormone production by the tumors (28). The use of radiolabeled somatostatin analogs has permitted imaging as well as therapy of neuroendocrine tumors and their metastases in patients (29). Similar targeting strategies have also been applied to vasoactive intestinal peptide receptors in epithelial tumors (30) and cholecystikinin-B receptors in medullary thyroid carcinomas and small cell lung cancers (31). Recently, we and other groups have labeled cyclic RGD peptides with various radionuclides for imaging of tumor angiogenesis (32,33). Overexpression of the G protein-coupled gastrin-releasing peptide (GRP) receptor in a variety of neoplasias, such as breast, prostatic, pancreatic and small cell lung cancers was prompted the

development of gamma-emitting or positron-emitting radionuclides labeled GRP analogs for SPECT (20-25,34) and PET (27) imaging of GRP receptor positive tumors.

Since the native bombesin peptide (BBN) has a pyroglutamic acid at the N-terminus and an amidated methionine at the C-terminus, further modification and radiolabeling of this peptide with metallic radionuclides is not possible. Efforts have been made to design derivatized BBN analogs for binding and pharmacokinetics studies. Because BBN agonists are generally preferable to BBN antagonists for receptor specific internalization, most BBN analogs with amidated C-terminus that have been developed are agonists. Because the C-terminus is directly involved in the specific binding interaction with the GRP receptor, the truncated C-terminal heptapeptide sequence Trp-Ala-Val-Gly-His-Leu-Met (BBN(8-14)) must be maintained or minimally substituted. Several strategies have been applied to develop radiometallated BBN-analogous conjugates. For example, the N-terminal Glp of BBN has been replaced by Pro and subsequently conjugated with DOTA and DTPA for ^{111}In labeling (35,36); Arg³ was substituted with Lys³ and a N₂S₂ ligand was attached to the Lys side chain ϵ -amino group for $^{99\text{m}}\text{Tc}$ labeling (22) or DOTA and DTPA attached to Lys³ of [Lys³,Ty⁴]BBN for ^{111}In labeling (35). Most of the studies reported to date used a C-terminal amidated BBN (8-14) in which radiometal chelate was linked to the truncated small peptide (37,38) for $^{99\text{m}}\text{Tc}$ labeling. Recently, Rogers et al (27) reported ^{64}Cu -labeled, DOTA-conjugated, 8-aminooctanoic acid (Aoc) linker modified BBN(7-14) for microPET imaging of subcutaneous PC-3 tumor models. The strategy used in our laboratory has focused primarily on modification of the Lys³ residue of [Lys³]BBN with various linkers and

chelators for diagnostic and therapeutic applications. This study reports ^{64}Cu -labeled DOTA-[Lys³]BBN for microPET imaging of both AI and AD tumor models.

In contrast to many other investigators who tried to conjugate DOTA chelator to peptides via solid-phase synthesis using DOTA-tris(*tert*-butyl ester) followed by TFA cleavage and deprotection, we found that the incorporation yield of tri-*tert*-butyl ester protected DOTA to fully protected peptides fixed on resin was low due to steric hindrance of the bulky protecting groups. Purification of the peptide conjugates was difficult due to the fact that DOTA-peptide conjugates usually had similar retention time to those of the parent peptides. We also found it more convenient to prepare DOTA-peptide conjugates in buffer solutions via *in situ* activation of DOTA. The retention time of DOTA-[Lys³]BBN is less 1 min different from that of [Lys³]BBN under the HPLC condition in this report. However, the use of an excess amount of DOTA for conjugation resulted in almost complete conversion of [Lys³]BBN to DOTA-[Lys³]BBN. The radiolabeling of DOTA-[Lys³]BBN with ^{64}Cu was performed with high yield. Unreacted copper-64 was easily removed by simple C₁₈ cartridge elution.

DOTA-[Lys³]BBN had high affinity for the GRP receptor ($\text{IC}_{50} = 2.2 \pm 0.5 \text{ nM}$, **Figure 2**) similar to that of bombesin (1.5 nM) (25). This study agrees with the findings by Baidoo et al (22) that modification of the Lys³ ϵ -amino group has little effect on the receptor binding characteristics of the peptide. ^{64}Cu -labeled DOTA-[Lys³]BBN was rapidly internalized by PC-3 cells, consistent with the expected agonistic behavior of this radiotracer against GRP receptor. Maximum internalization and retention of the

radioactivity by tumor cells is needed for diagnostic and/or therapeutic efficacy of radiopharmaceuticals. There was limited efflux of ^{64}Cu activity from the PC-3 cells within the period of investigation (2 h), presumably due to residualization of ^{64}Cu from GRP receptor mediated entrapment of the tracer in lysosomes (39,40) and subsequent degradation by lysosomal proteases. Similar results have been obtained with other radiolabeled BBN analogs.

Biodistribution studies were performed on both PC-3 (AI) and CWR22 (AD) tumor-bearing mice. It has been reported that AI tumor cells express GRP receptors at significantly higher levels than do AD tumor cells (16). In the current study, activity accumulation from ^{64}Cu -DOTA-[Lys³]BBN by AI PC-3 tumors was significantly higher than by AD CWR22 tumors. It is interesting to notice that receptor blocking did not reduce the uptake in CWR22 tumor, whereas the activity in GRP receptor positive PC-3 tumor and pancreas were effectively inhibited. Fast blood clearance of radiotracer after 30 min postadministration might have been due to little binding of the degradation metabolites to plasma proteins. This is very different from the *in vivo* behavior of ^{64}Cu -DOTA-Aoc-BBN(7-14) (27), which exhibited persistent blood retention up to 24 h postinjection, and higher normal tissue uptake than that reported in this and other studies. A high degree of plasma protein binding of the relatively lipophilic Aoc linker as well as transchelation of Cu^{2+} to albumin and superoxide dismutase may have caused the unfavorably high liver activity accumulation. Smith et al. (38) also reported that a long aliphatic linker is responsible for prolonged retention in blood and decreased pancreatic uptake.

Although ^{99m}Tc -labeled GRP analogs have receptor specific tumor activity accumulation, the absolute tumor uptake is rather low (less than 1% %ID/g at 1 h postinjection). ^{64}Cu -labeled BBN analogs reported here and by Rogers et al (27) gave much higher tumor uptake and more persistent tumor retention. Further investigations are needed to fully understand the effect of radiochelate characteristics, linker properties, and peptide sequences on tumor targeting ability and excretion kinetics. As opposed to ^{64}Cu -DOTA-Aoc-BBN(7-14), which had both hepatobiliary and renal excretion pathways, ^{64}Cu -DOTA-[Lys³]BBN was excreted rapidly via the renal route. This suggests that insertion of a rather hydrophobic aliphatic acid linker to separate the radiolabel from the receptor targeting peptide moiety is probably not beneficial for optimization of such radioligands.

MicroPET imaging of ^{64}Cu -DOTA-[Lys³]BBN in mice bearing both AI PC-3 and AD CWR22 tumors 1 h after injection of radioactivity revealed high tumor-to-background ratio for both tumor types (**Figure 6**). The uptake indices found with microPET and QAR for PC-3 tumor and pancreas were significantly lower than those obtained from direct tissue sampling (**Figure 7**). Assuming the specific activity of the radiotracer to have been 500 mCi/ μmol at the time of tail vein injection, the injection administered for microPET imaging contained about 2 μg BBN peptide (400 μCi), while the amount of activity administered for the biodistribution experiment contained only 50 ng BBN peptide (10 μCi). It is possible that partial self-inhibition of receptor specific uptake in PC-3 tumor, pancreas and other tissues that express the GRP receptor occurred during the imaging studies. Conversely, the inability to inhibit CWR22 tumor activity accumulation in the

imaging study is consistent with the known low GRP receptor expression in androgen-dependent tumors such as CWR22 (16).

We anticipate that quantitative imaging with microPET in living animals, based upon the overexpression of GRP receptor in invasive prostate cancer, could potentially be translated into clinical settings to detect androgen-independent prostate cancer. Successful targeting of this molecular pathway would have diagnostic, as well as potential radio- and chemo-therapeutic implications. The ability to document GRP receptor density and the appropriate selection of patients entering clinical trials for anti-GRP receptor treatment. PET imaging of prostate cancer with ^{64}Cu -labeled bombesin analogs will be useful for determining dosimetry and tumor response to the same ligand labeled with therapeutic amounts of ^{67}Cu for internal radiotherapy.

CONCLUSION

[Lys³]BBN when conjugated with a macrocyclic DOTA chelating group and radiolabeled with the positron emitting radionuclide copper-64 exhibits high GRP receptor binding affinity and specificity and rapid internalization in androgen-independent PC-3 prostate cancer cells. Specific localization of ⁶⁴Cu-DOTA-[Lys³]BBN to PC-3 tumor and GRP receptor positive tissues was confirmed by biodistribution, microPET imaging and autoradiographic imaging studies. Reduced tumor uptake in PC-3 tumor but not CWR22 tumor in high dose microPET and autoradiography studies compared to low dose biodistribution studies further illustrates high affinity and low capacity characteristics of the GRP receptor in AI tumors. The activity accumulation in CWR22 tumor is attributed to non-specific uptake. Further studies to evaluate the metabolic stability and optimization of the radiotracers for prolonged tumor retention and improved in vivo kinetics is currently in progress.

ACKNOWLEDGMENTS

This work was funded by the DOD Prostate Cancer Research Program DAMD17-03-1-0143 (X.C.) and NIH grant P20 CA86532 (P.S.C.). Production of Cu-64 at Washington University School of Medicine was supported by the NCI grant R24 CA86307.

REFERENCES

1. Effert PJ, Bares R, Handt S, Wolff JM, Bull U, Jakse G. Metabolic imaging of untreated prostate cancer by positron emission tomography with ^{18}F -labeled deoxyglucose. *J Urol*. 1996;155:994-998.
2. Liu IJ, Zafar MB, Lai YH, Segall GM, Terris MK. Fluorodeoxyglucose positron emission tomography studies in diagnosis and staging of clinically organ-confined prostate cancer. *Urology*. 2001;57:108-111.
3. Hara T, Kosaka N, Kishi H. PET imaging of prostate cancer using carbon-11-choline. *J Nucl Med*. 1998;39:990-995.
4. Kotzerke J, Prang J, Neumaier B, et al. Experience with carbon-11 choline positron emission tomography in prostate carcinoma. *Eur J Nucl Med*. 2000;27:1415-1419.
5. Price DT, Coleman RE, Liao RP, Robertson CN, Polascik TJ, DeGrado TR. Comparison of [^{18}F]fluorocholine and [^{18}F]fluorodeoxyglucose for positron emission tomography of androgen dependent and androgen independent prostate cancer. *J Urol*. 2002;168:273-280.
6. DeGrado TR, Baldwin SW, Wang S, et al. Synthesis and evaluation of ^{18}F -labeled choline analogs as oncologic PET tracers. *J Nucl Med*. 2001;42:1805-1814.
7. DeGrado TR, Coleman RE, Wang S, et al. Synthesis and evaluation of ^{18}F -labeled choline as an oncologic tracer for positron emission tomography: initial findings in prostate cancer. *Cancer Res*. 2001;61:110-117.

8. Hara T, Kosaka N, Kishi H. Development of ^{18}F -fluoroethylcholine for cancer imaging with PET: synthesis, biochemistry, and prostate cancer imaging. *J Nucl Med*. 2002;43:187-199.
9. Kotzerke J, Volkmer BG, Neumaier B, Gschwend JE, Hautmann RE, Reske SN. Carbon-11 acetate positron emission tomography can detect local recurrence of prostate cancer. *Eur J Nucl Med Mol Imaging*. 2002;29:1380-1384.
10. Kato T, Tsukamoto E, Kuge Y, et al. Accumulation of [^{11}C]acetate in normal prostate and benign prostatic hyperplasia: comparison with prostate cancer. *Eur J Nucl Med Mol Imaging*. 2002;29:1492-1495.
11. Oyama N, Akino H, Kanamaru H, et al. ^{11}C -acetate PET imaging of prostate cancer. *J Nucl Med*. 2002;43:181-186.
12. Oyama N, Miller TR, Dehdashti F, et al. ^{11}C -acetate PET imaging of prostate cancer: detection of recurrent disease at PSA relapse. *J Nucl Med*. 2003;44:549-555.
13. Bonasera TA, O'Neil JP, Xu M, et al. Preclinical evaluation of fluorine-18-labeled androgen receptor ligands in baboons. *J Nucl Med*. 1996;37:1009-1015.
14. Markwalder R, Reubi JC. Gastrin-releasing peptide receptors in the human prostate: relation to neoplastic transformation. *Cancer Res*. 1999;59:1152-1159.
15. Sun B, Halmos G, Schally AV, Wang X, Martinez M. Presence of receptors for bombesin/gastrin-releasing peptide and mRNA for three receptor subtypes in human prostate cancers. *Prostate*. 2000;42:295-303.
16. Reile H, Armatis PE, Schally AV. Characterization of high-affinity receptors for bombesin/gastrin releasing peptide on the human prostate cancer cell lines PC-3

- and DU-145: internalization of receptor bound ^{125}I -(Tyr⁴) bombesin by tumor cells. *Prostate*. 1994;25:29-38.
17. Jongsma J, Oomen MH, Noordzij MA, et al. Androgen-independent growth is induced by neuropeptides in human prostate cancer cell lines. *Prostate*. 2000;42:34-44.
 18. Szepeshazi K, Halmos G, Schally AV, et al. Growth inhibition of experimental pancreatic cancers and sustained reduction in epidermal growth factor receptors during therapy with hormonal peptide analogs. *J Cancer Res Clin Oncol*. 1999;125:444-452.
 19. Schally AV, Comaru-Schally AM, Plonowski A, Nagy A, Halmos G, Rekasi Z. Peptide analogs in the therapy of prostate cancer. *Prostate*. 2000;45:158-166.
 20. Van de Wiele C, Dumont F, Dierckx RA, et al. Biodistribution and dosimetry of $^{99\text{m}}\text{Tc}$ -RP527, a gastrin-releasing peptide (GRP) agonist for the visualization of GRP receptor-expressing malignancies. *J Nucl Med*. 2001;42:1722-1727.
 21. Van de Wiele C, Dumont F, Vanden Broecke R, et al. Technetium-99m RP527, a GRP analogue for visualisation of GRP receptor-expressing malignancies: a feasibility study. *Eur J Nucl Med*. 2000;27:1694-1699.
 22. Baidoo KE, Lin KS, Zhan Y, Finley P, Scheffel U, Wagner HN Jr. Design, synthesis, and initial evaluation of high-affinity technetium bombesin analogues. *Bioconjug Chem*. 1998;9:218-225.
 23. Karra SR, Schibli R, Gali H, et al. $^{99\text{m}}\text{Tc}$ -labeling and in vivo studies of a bombesin analogue with a novel water-soluble dithiadiphosphine-based bifunctional chelating agent. *Bioconjug Chem*. 1999;10:254-260.

24. La Bella R, Garcia-Garayoa E, Langer M, Blauenstein P, Beck-Sickinger AG, Schubiger PA. In vitro and in vivo evaluation of a $^{99m}\text{Tc(I)}$ -labeled bombesin analogue for imaging of gastrin releasing peptide receptor-positive tumors. *Nucl Med Biol.* 2002;29:553-560.
25. La Bella R, Garcia-Garayoa E, Bahler M, et al. A $^{99m}\text{Tc(I)}$ -postlabeled high affinity bombesin analogue as a potential tumor imaging agent. *Bioconjug Chem.* 2002;13:599-604.
26. Wu AM, Yazaki PJ, Tsai S, et al. High-resolution microPET imaging of carcinoembryonic antigen-positive xenografts by using a copper-64-labeled engineered antibody fragment. *Proc Natl Acad Sci USA.* 2000;97:8495-8500.
27. Rogers BE, Bigott HM, McCarthy DW, et al. MicroPET imaging of a gastrin-releasing peptide receptor-positive tumor in a mouse model of human prostate cancer using a ^{64}Cu -labeled bombesin analogue. *Bioconjug Chem.* 2003;14:756-763.
28. Lamberts SW, Krenning EP, Reubi JC. The role of somatostatin and its analogs in the diagnosis and treatment of tumors. *Endocr Rev.* 1991;12:450-482.
29. Breeman WA, de Jong M, Kwekkeboom DJ, et al. Somatostatin receptor-mediated imaging and therapy: basic science, current knowledge, limitations and future perspectives. *Eur J Nucl Med.* 2001;28:1421-1429.
30. Virgolini I, Raderer M, Kurtaran A, et al. Vasoactive intestinal peptide-receptor imaging for the localization of intestinal adenocarcinomas and endocrine tumors. *N Engl J Med.* 1994;331:1116-1121.

31. Behr TM, Jenner N, Radetzky S, et al. Targeting of cholecystokinin-B/gastrin receptors in vivo: preclinical and initial clinical evaluation of the diagnostic and therapeutic potential of radiolabelled gastrin. *Eur J Nucl Med*. 1998;25:424-430.
32. Chen X, Park R, Shahinian AH, et al. ¹⁸F-Labeled RGD peptide: initial evaluation for imaging brain tumor angiogenesis. *Nucl Med Biol*. 2004;31:in press.
33. Haubner R, Wester HJ, Weber WA, et al. Noninvasive imaging of $\alpha_v\beta_3$ integrin expression using ¹⁸F-labeled RGD-containing glycopeptide and positron emission tomography. *Cancer Res*. 2001;61:1781-1785.
34. Smith CJ, Volkert WA, Hoffman TJ. Gastrin releasing peptide (GRP) receptor targeted radiopharmaceuticals: A concise update. *Nucl Med Biol*. 2003;30:861-868.
35. Breeman WA, de Jong M, Erion JL, et al. Preclinical comparison of ¹¹¹In-labeled DTPA- or DOTA-bombesin analogs for receptor-targeted scintigraphy and radionuclide therapy. *J Nucl Med*. 2002;43:1650-1656.
36. Breeman WA, De Jong M, Bernard BF, et al. Pre-clinical evaluation of [¹¹¹In-DTPA-Pro¹, Tyr⁴]bombesin, a new radioligand for bombesin-receptor scintigraphy. *Int J Cancer*. 1999;83:657-663.
37. Hoffman TJ, Gali H, Smith CJ, et al. Novel series of ¹¹¹In-labeled bombesin analogs as potential radiopharmaceuticals for specific targeting of gastrin-releasing peptide receptors expressed on human prostate cancer cells. *J Nucl Med*. 2003;44:823-831.

38. Smith CJ, Gali H, Sieckman GL, Higginbotham C, Volkert WA, Hoffman TJ. Radiochemical investigations of $^{99m}\text{Tc-N}_3\text{S-X-BBN}[7-14]\text{NH}_2$: an in vitro/in vivo structure-activity relationship study where X = 0-, 3-, 5-, 8-, and 11-carbon tethering moieties. *Bioconjug Chem.* 2003;14:93-102.
39. Slice LW, Yee HF Jr, Walsh JH. Visualization of internalization and recycling of the gastrin releasing peptide receptor-green fluorescent protein chimera expressed in epithelial cells. *Receptors Channels.* 1998;6:201-212.
40. Grady EF, Slice LW, Brant WO, Walsh JH, Payan DG, Bunnett NW. Direct observation of endocytosis of gastrin releasing peptide and its receptor. *J Biol Chem.* 1995;270:4603-4611.

Figure Captions

Figure 1. Schematic structures of DOTA-[Lys³]BBN conjugate and ⁶⁴Cu-DOTA-[Lys³]BBN.

Figure 2. Inhibition of ¹²⁵I-[Tyr³]BBN binding to the GRP receptor on human prostate cancer cell line PC-3 by DOTA-[Lys³]BBN conjugate (IC₅₀ = 2.2 ± 0.1 nM). Results expressed as percentage of binding are mean ± SD of 2 experiments in triplicate.

Figure 3. Time-dependent internalization of ⁶⁴Cu-DOTA-[Lys³]BBN by PC-3 prostate cancer cells incubated at 37°C during 2 h. The cells were pre-incubated for 2 h at 4 °C. The data are mean ± SD of the percentage of acid-resistant (internalized) radioactivity in the cells (2 experiments in triplicate).

Figure 4. Biodistribution of ⁶⁴Cu-DOTA-[Lys³]BBN in male athymic nude mice bearing s.c. PC-3 (AI) and CWR22 (AD) tumors. Mice were intravenously injected with 10 µCi of radioligand and sacrificed at 15 min, 30 min, 1 h, 2 h and 4 h. The data are presented as mean % ID/g ± SD (n = 4). Sm int = small intestine.

Figure 5. Receptor blocking study: biodistribution of ⁶⁴Cu-DOTA-[Lys³]BBN at 1 h time point without (white bars) and with (black bars) co-injection of 200 µg of BBN to determine GRP receptor specific binding. Significant inhibition of activity accumulation in PC-3 tumor ($p < 0.001$) and pancreas ($p < 0.001$) were observed. Data are presented as

mean % ID/g \pm SD in reference to total injected dose of the radiotracer (n = 4 for each group).

Figure 6. Left: Coronal microPET image of tumor bearing mouse (PC-3 on the right shoulder and CWR22 on the right shoulder) 1 h after administration of ^{64}Cu -DOTA-[Lys³]BBN. Right: Digital autoradiograph of the section containing tumors.

Figure 7. Kidney, liver, PC-3 tumor and CWR22 tumor uptake comparison as obtained from traditional biodistribution (n = 4), microPET (n = 3), and autoradiographic quantification (n = 3). Quantification of microPET and autoradiography revealed similar activity accumulation in both PC-3 tumor and pancreas, which were both lower than those obtained from biodistribution study.

Figure 8. Transaxial microPET images of an athymic nude mouse bearing PC-3 tumor on the right shoulder 1 h after tail vein injection of 400 μCi ^{64}Cu -DOTA-[Lys³]BBN in the absence (control) or presence (block) of co-injected blocking dose of BBN (10 mg/kg).

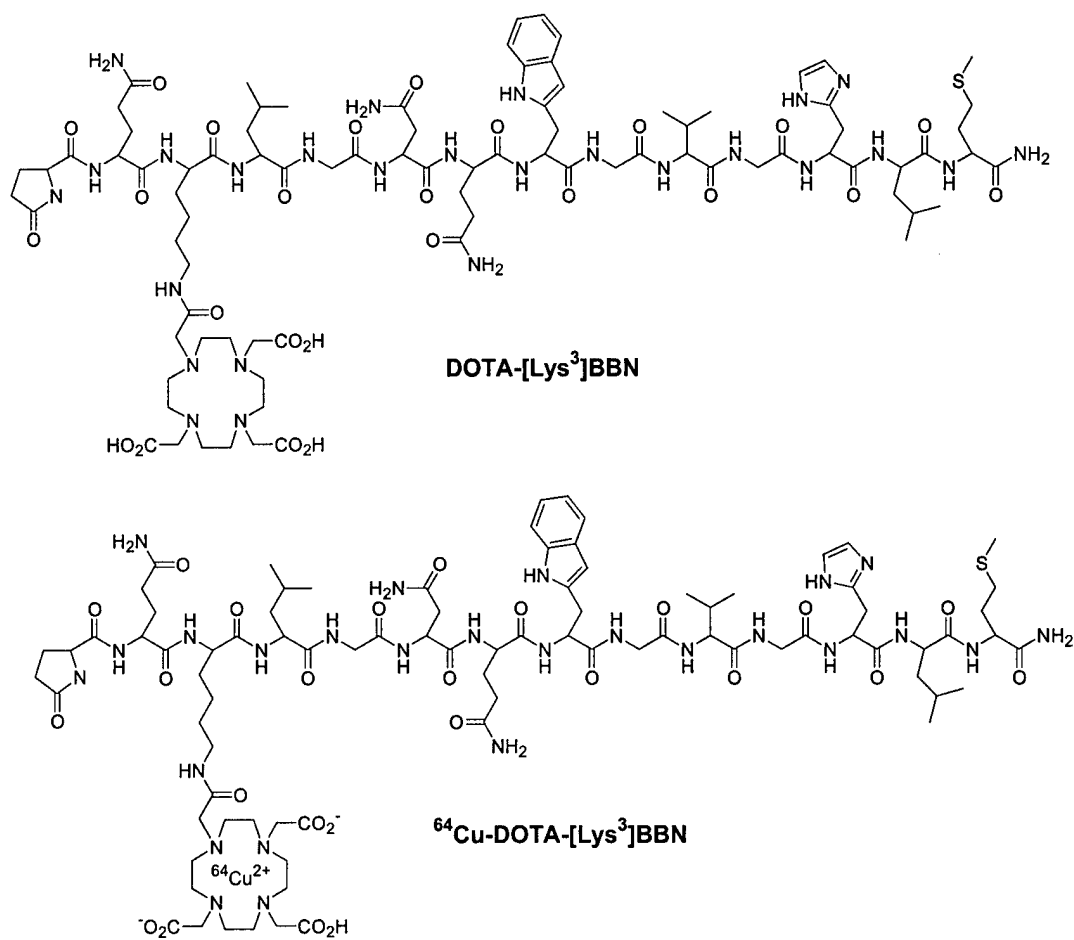


Fig. 1

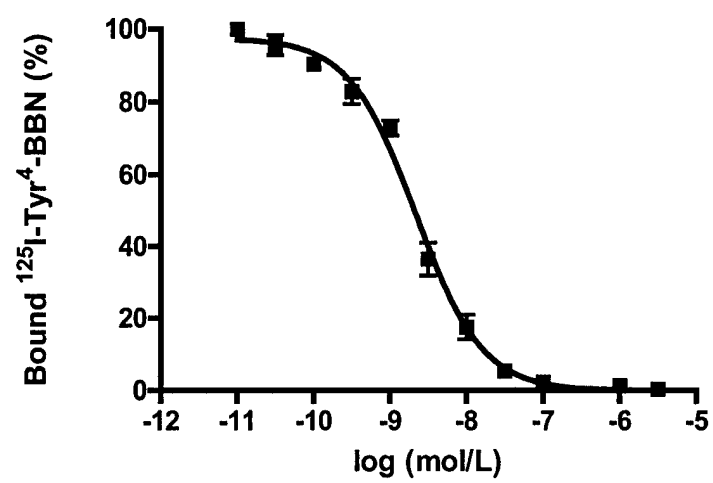


Fig. 2

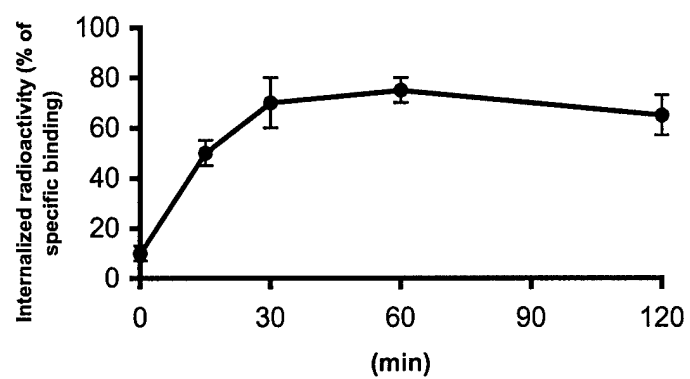


Fig. 3

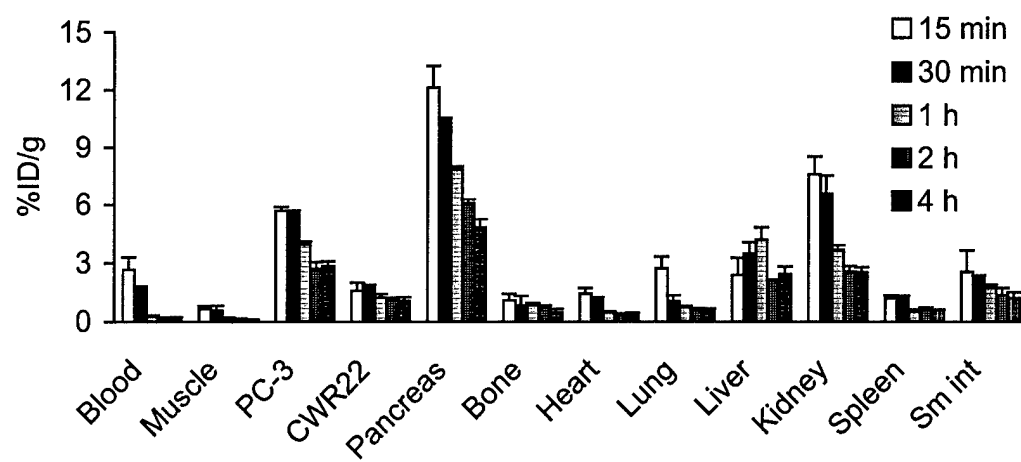


Fig. 4

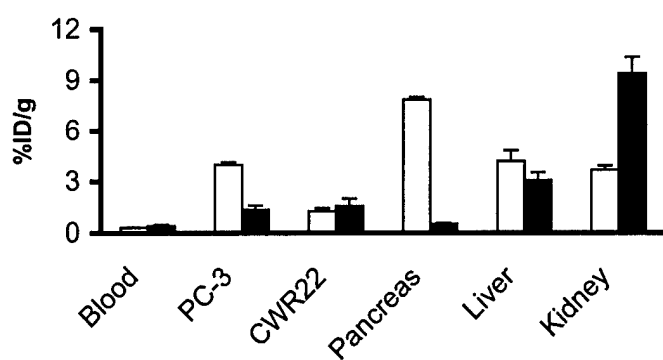


Fig. 5

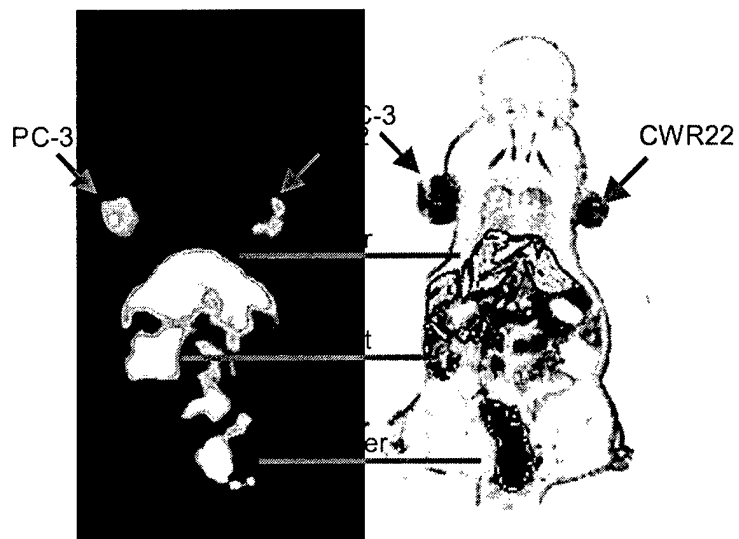


Fig. 6

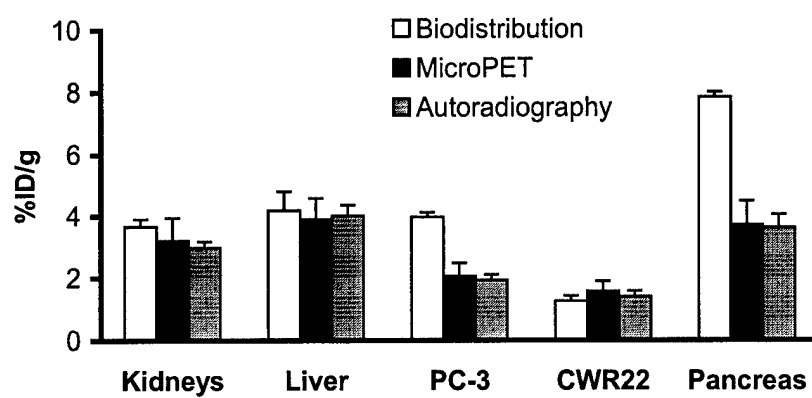


Fig. 7

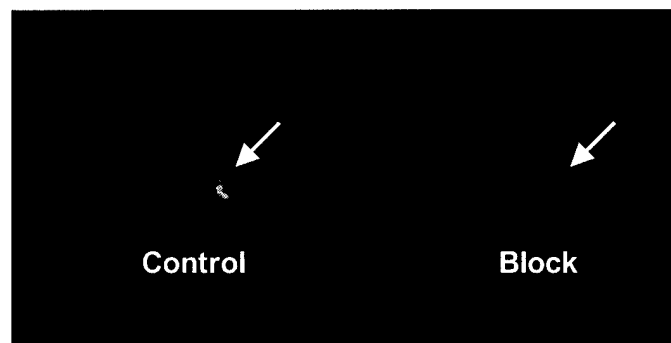


Fig. 8

Evaluation of ^{64}Cu -Labeled $[\text{Lys}^3]\text{Bombesin}$ as PET Tracer for Prostate Cancer GRP Receptor Imaging

X. Chen, Y. Hou, R. Park, M. Tohme, A. H. Shahinian, J. R. Bading, P. S. Conti;
University of Southern California, Los Angeles, CA.

Overexpression of gastrin-releasing peptide (GRP) receptor in both androgen-dependent (AD) and androgen-independent (AI) human neoplastic prostate tissues provides an attractive target for prostate cancer imaging and therapy. The goal of this study is to develop ^{64}Cu -radiolabeled GRP analogs for positron emission tomography (PET) imaging of GRPR expression in prostate cancer xenografted mice. Lys^3 -bombesin ($[\text{Lys}^3]\text{BBN}$) was conjugated with 1,4,7,10-tetraazadodecane- N,N',N'',N''' -tetraacetic acid (DOTA) and labeled with positron emitter ^{64}Cu . Competitive receptor binding assay using PC-3 cells against ^{125}I - $[\text{Tyr}^4]\text{BBN}$ revealed an IC_{50} value of 2.2 ± 0.5 nM for DOTA- $[\text{Lys}^3]\text{BBN}$. Incubation of the ^{64}Cu -labeled radiotracer showed temperature- and time-dependent internalization. The radiotracer revealed higher uptake in AI PC-3 tumor (5.62 ± 0.08 %ID/g at 30 min p.i.) than in AD 22Rv1 tumor (1.75 ± 0.05 %ID/g at 30 min p.i.). Significant accumulation of the activity in GRPR positive pancreas was also observed (10.4 ± 0.15 %ID/g at 30 min p.i.). Co-injection of blocking dose of $[\text{Lys}^3]\text{BBN}$ inhibited the activity accumulation in PC-3 tumor and pancreas but not in 22Rv1 tumor. MicroPET and autoradiographic imaging of ^{64}Cu -DOTA- $[\text{Lys}^3]\text{BBN}$ in athymic nude mice bearing subcutaneous PC-3 and 22Rv1 tumors showed strong tumor-to-background contrast. This study demonstrates that ^{64}Cu -DOTA- $[\text{Lys}^3]\text{BBN}$ is able to detect GRPR-positive prostate cancer by PET imaging. Further studies to evaluate the metabolic stability and optimization of the radiotracers for prolonged tumor retention and improved *in vivo* kinetics is currently in progress [This work was funded by DOD Prostate Cancer Research Program DAMD17-03-1-0143 (X.C.) and NIH grant P20 CA86532 (P.S.C.). The production of Cu-64 at Washington University was supported by NCI grant R24 CA86307].